Published in final edited form as:
Hippocampus. 2012 November ; 22(11): 2184–2198. doi:10.1002/hipo.22038.

Modulation by pregnenolone sulfate of filtering properties in the hippocampal trisynaptic circuit

Chessa S. Scullin[1,2] and **L. Donald Partridge**[1]

[1]Department of Neurosciences, University of New Mexico, Albuquerque, NM 87131

[2]Joint BioEnergy Institute, Physical Biosciences Division, Lawrence Berkeley National Laboratory, Emeryville, CA 94608, Sandia National Laboratories, Biomass Science and Conversion Technology Department, Livermore, CA 94550

Abstract

Short-term synaptic plasticity alters synaptic efficacy on a timescale that is relevant to encoding information in spike trains. The dynamics of this plasticity, combined with that of the feedback and feedforward contributions of local interneurons, impose frequency-dependent properties on neuronal networks with implications for nervous system function. The trisynaptic network of the hippocampus is especially well suited to selectively filter components of frequency-dependent signals that are transmitted from the entorhinal cortex. We measured presynaptic $[Ca^{2+}]_i$ in perforant path, mossy fiber, or Schaffer collateral terminals while simultaneously measuring field potentials of principal cells of the dentate, CA3, or CA1 synaptic fields over a range of stimulus frequencies of 2 to 77 Hz. In all three synaptic fields, the average $[Ca^{2+}]_i$ during a 500 ms stimulus train rose monotonically with stimulus frequency. The average population spike amplitude during this stimulus train, however, exhibited a non-linear relationship to frequency that was distinct for each of the three synaptic fields. The dentate synaptic field exhibited the characteristics of a low pass filter, while both CA synaptic fields had bandpass filter characteristics with a gain that was greater than 1 in the passband frequencies. Importantly, alteration of the dynamic properties of this network could significantly impact information processing performed by the hippocampus. Pregnenolone sulfate (PregS), has frequency-dependent effects on paired- and multi-pulse plasticity in the dentate and CA1 synaptic fields of the hippocampal formation. We investigated the PregS-dependent modulation of the dynamic properties of transmission by the principal cells of the three hippocampal synaptic fields. Importantly, PregS is capable of altering the pattern separation capabilities that may underlie hippocampal information processing.

Keywords

gamma; theta; bandpass filter; lowpass filter; neurosteroid

Introduction

Neuronal information processing

Long-term synaptic plasticity is generally accepted to be the cellular underpinning of learning and memory (Bliss and Collingridge, 1993). By contrast, short-term synaptic plasticity may be important for working memory (Deng and Klyachko, 2011; Mongillo et al., 2008) and it certainly alters synaptic efficacy on a timescale that is relevant to encoding

Corresponding Author: L. Donald Partridge, Department of Neurosciences, University of New Mexico School of Medicine, Albuquerque, New Mexico, 87131, USA, dpartridge@salud.unm.edu.

information in spike trains (Dittman et al., 2000). The dynamics of short-term synaptic plasticity, combined with dynamic properties of the feedback and feedforward contributions of local networks, generate frequency-dependent properties that filter information transfer through neuronal networks. In particular, the classic trisynaptic network of the hippocampus is especially well suited to selectively filter components of signals, particularly those in the θ and γ frequency bands, which are transmitted from the entorhinal cortex. Importantly, modulation of the dynamic properties of this network could significantly impact information processing performed by the hippocampus.

Trisynaptic circuit of the hippocampal formation

The intrinsic connections of the hippocampal formation from entorhinal cortex to dentate to CA3 and then to CA1 produce the well characterized trisynaptic circuit that was described in the classic histological studies of Cajal and Lorente de Nó and subsequently in numerous electrophysiological studies (e.g. (Andersen, 1975)). In addition to their input role in this classic circuit, projections from the entorhinal cortex also provide more minor inputs to CA3 pyramidal neurons (Freund and Buzsaki, 1996) and to distal dendrites of CA1 pyramidal neurons (Ahmed and Mehta, 2009; Speed and Dobrunz, 2009).

Oscillatory activity in hippocampal synaptic fields is sculpted through the action of numerous modulatory receptors including nicotinic ACh receptors (Griguoli and Cherubini, 2011), μ-opioid receptors (Gulyas et al., 2010), histamine H_3 receptors (Andersson et al., 2010), metabotropic glutamate receptors (Traub et al., 2005), and cannabinoid CB_1 receptors (Holderith et al., 2011). In addition, both feedforward and feedback processing of firing frequency occur in each of the three hippocampal synaptic fields through the action of local GABAergic interneurons.

Frequency response properties of neuronal firing

Theta (θ, 4 – 8 Hz) and gamma (γ, 30 – 100 Hz) frequencies are especially significant for information processing in the hippocampus with θ frequencies important for place cell encoding (O'Keefe and Recce, 1993) and γ frequencies playing a role in attention (Colgin et al., 2009). It has been shown that at least certain spectral bands can be correlated with multiunit spiking activity (Whittingstall and Logothetis, 2009) to reflect activity in local neuronal networks (Okun et al., 2010). In his extensive description of the hippocampal trisynaptic circuit, Andersen observed that an increasing stimulation rate of perforant path fibers is necessary to generate responses first in dentate granule cells and then in CA3 pyramidal neurons and finally in CA1 pyramidal neurons. As a result, he noted that "varying the input frequency may determine to what degree the impulses traverse the multi-neuronal loop" (Andersen, 1975). Subsequently, it was observed that high frequency firing patterns recorded as animals traversed place fields were those that were best transmitted from dentate granule cells to CA3 pyramidal neurons (Henze et al., 2002). Thus the frequency response properties imparted by synaptic mechanisms and interneuronal feedforward and feedback connections are clearly important to the effectiveness of information transfer between the hippocampal synaptic fields.

Frequency-dependent contributions of neurosteroids

Sulfated neuroactive steroids, which may be produced in the brain and act locally on neurons, play important roles in both normal and pathological functions of the nervous system with involvement in such widespread areas as learning and memory, epilepsy, stress, and depression (Gibbs et al., 2006; Reddy, 2010). Pregnenolone sulfate (PregS) is an important member of this group that has well characterized postsynaptic actions on ionotropic and metabotropic receptors as well as on voltage-gated channels (Kobayashi et al., 2009). In addition, PregS has been shown to have presynaptic effects in modulating the

release of several neurotransmitters (Valenzuela et al., 2008; Zheng, 2009). Importantly, we have shown that, at physiologically relevant concentrations, PregS acts presynaptically, to modulate glutamatergic transmission at both perforant path-to-dentate granule cell synapses (Thomas et al., 2005) and at Schaffer collateral-to-CA1 pyramidal neuron synapses (Partridge and Valenzuela, 2001; Partridge and Valenzuela, 2002).

PregS directly affects the frequency dependency of hippocampal long term synaptic plasticity (Chen et al., 2010) and plays an important role in hippocampus-dependent spatial learning (Vallee et al., 1997). The effects of PregS in both the dentate and CA1 are dependent upon the stimulation frequency in a manner that is unique to each of these synaptic fields. In the dentate synaptic field, PregS acts as a pattern separation filter that emphasizes signals in the θ range at the expense of those in the γ range (Thomas et al., 2005) while in the CA1 synaptic field, PregS action would favor complex spikes within the γ frequency range over signals in the θ frequency range (Partridge and Valenzuela, 2002). As θ and γ frequencies are important for place cell encoding (Lisman, 2005), a more complete investigation of the influence of PregS on the transmission of these frequencies can increase our understanding of the action of neurosteroids in hippocampal signal processing.

In this study, we undertook a more extensive investigation of the dynamic plastic properties of each of the synaptic fields in the classic hippocampal trisynaptic circuit with the goal of better understanding the mechanisms that underlie both synaptic and network filtering properties and, additionally, the effects of the neurosteroid PregS on these important signal modulating processes.

Materials and Methods

Slice preparation

Experiments were performed in coronal hippocampal slices prepared from approximately 50 day old Sprague-Dawley rats as previously described (Scullin and Partridge, 2010). Briefly, animals were deeply anaesthetized by i.p. injection of 250 mg kg^{-1} ketamine (Fort Dodge Animal Health, Fort Dodge, IA, USA), brains were rapidly removed, and slices were cut at 300 μm with a vibroslicer (Pelco 101, St Louis, MO, USA) in an ice bath with a cutting solution containing (mM): 220 sucrose, 3 KCl, 1.2 NaH_2PO_4, 26 $NaHCO_3$, 12 $MgSO_4$, 0.2 $CaCl_2$, 10 glucose and 0.01 mg ml^{-1} ketamine equilibrated with 95%O_2–5%CO_2. Slices were then transferred to a bath containing artificial cerebrospinal fluid (ACSF) containing (mM): 126 NaCl, 3 KCl, 1.25 NaH_2PO_4, 1.3 $MgSO_4$, 26 $NaHCO_3$, 2.5 $CaCl_2$ and 10 glucose equilibrated with 95%O_2–5%CO_2 at 30°C for 1 h and then maintained at room temperature until transfer to a temperature-controlled recording chamber (Warner Instruments, Hamden, CT, USA), which was maintained at 32°C and continuously perfused at 2 ml min^{-1} with ACSF saturated with 95%O_2–5%CO_2. All experiments were approved by the Institutional Animal Care and Use Committee at the University of New Mexico Health Sciences Center and conformed with NIH guidelines.

Presynaptic Ca^{2+} imaging

Presynaptic fibers were filled with the Ca^{2+} fluorophore, Mg Green AM (Molecular Probes, Eugene, OR, USA) using an established technique that permits measurement of a spatial and temporal average of $[Ca^{2+}]_i$ of the presynaptic terminal (Regehr et al., 1994; Scullin and Partridge, 2010) and allows simultaneous measurements of presynaptic $[Ca^{2+}]_i$ and postsynaptic field potentials in localized populations of synaptic contacts. To minimize the effect of competition with endogenous Ca^{2+} buffers, we used Mg-Green, with a Ca^{2+} binding K_D = 6 μM (Atluri and Regehr, 1996; Regehr and Atluri, 1995). An ejection

electrode (tip diameter 5 – 10 μm) containing the fluorophore (0.9 mM Mg Green AM, 10% DMSO, 1% pluronic acid in ACSF) was lowered into the appropriate fiber pathway between the stimulating electrode and the presynaptic terminal field to be investigated. While observing the emission image at the 490 nm excitation wavelength, an air pressure pulse was applied to the ejection electrode with a syringe until a small bright spot (≈1 μl) was observed in the presynaptic fiber pathway.

The slice was then maintained with a 2 ml min^{-1} flow of oxygenated ACSF at 32°C for 1 h to allow intracellular diffusion of the dye to the presynaptic imaging site approximately 500 μm away from the ejection site. The excitation light was then reduced to a 100–200 μm diameter spot with a diaphragm in the epi-illumination path, and the emitted light was measured with a photomultiplier tube (PMT). This spot included, or was immediately adjacent to, the area electrically summed by the field potential recording.

The localization of the $\Delta F/F_0$ response to the presynaptic terminals of the input fibers of the synaptic field was verified with the following two control experiments (Schiess et al., 2006). First, in the presence of 10 μM CNQX, 25 μM D-AP5, and 20 μM bicuculline, the fEPSP (field excitatory postsynaptic potential), but not the presynaptic fiber volley, was blocked while the $\Delta F/F_0$ signal was left essentially unchanged. Second, the subsequent addition of 600 nM TTX blocked both the $\Delta F/F_0$ signal and the presynaptic fiber volley.

Fluorescence responses are reported as the ratio of the change in fluorescence to the pre-stimulus fluorescence ($\Delta F/F_0$), corrected for bleaching by subtraction of a linearly sloping baseline, and inverted so that increasing presynaptic $[Ca^{2+}]_i$ produced an upward deflection. To diminish noise inherent with the use of the low-affinity Ca^{2+} indicator, it was necessary to average two fluorescence responses and to low pass filter the PMT signal at 1 kHz.

Presynaptic stimuli were delivered orthodromically by a Master 8 pulse generator (AMPI Instruments, Jerusalem, Israel) under control of the imaging system (TILL Photonics, Pleasanton, CA, USA). Two stimulus paradigms were used for measuring frequency responses of hippocampal synaptic fields. In the fixed frequency train paradigm, which was used in the majority of the experiments, 500 ms stimulus trains at frequencies between 2 and 77 Hz were applied in a sequence of either increasing or decreasing frequency. In the random instantaneous frequency paradigm, which was used in the experiment of figure 3, a stimulus train was applied that produced a random sequence of instantaneous frequencies between 2 and 77 Hz. The uniform distribution of instantaneous frequencies for a 40 s period of the random instantaneous frequency paradigm was determined by the following statistical tests: A Pearson's correlation of instantaneous frequency vs. time yielded $P = 0.383$ and $R^2 = 0.0279$ and a Spearman's correlation of the number of occurrences vs. binned instantaneous frequency yielded $P = 0.340$ and $R^2 = 0.0964$. A paired pulse paradigm at 50 ms interpulse interval over a range of stimulus intensities was used to generate figure 5A.

Field potential recordings

We used standard electrophysiological techniques for slice fEPSP recordings in the three synaptic fields of the hippocampal trisynaptic circuit (Schiess et al., 2006). The stimulating electrode was placed in the infrapyramidal blade of the dentate gyrus to stimulate lateral perforant pathway fibers for recordings in the dentate granule layer; in the *stratum lucidum* to stimulate mossy fibers for recordings in the *stratum pyramidale* of CA3; and in *stratum radiatum* to stimulate Schaffer collateral fibers for recordings in *stratum pyramidale* of CA1. Field potentials were recorded with a Multiclamp 700B amplifier (Molecular Devices, Sunnyvale, CA, USA) and a Digidata 1322A interface using pCLAMP 10 software (Molecular Devices) for experimental control and data analysis, digitized at 20 kHz, and

filtered at 2 kHz. Presynaptic constant current pulses (150 μs duration) were applied through a concentric bipolar electrode (FHC, Bowdoinham, ME, USA) from a Master 8 and an Iso-Flex constant current stimulator (both from API Instruments, Jerusalem, Israel) at a current, which was adjusted to produce 40–60% of the maximum fEPSP population spike (PS) amplitude.

In some instances, stable $\Delta F/F_0$ data or complete time or frequency records of fEPSP data were not successfully recorded; however, the remaining data were included in the analyses. As a result, there are differences in the numbers of slices given in figures 1 and 2 for each of the synaptic fields.

Modeling and Data analysis

Presynaptic residual $[Ca^{2+}]_i$ ($[Ca^{2+}]_{res}$) and postsynaptic PSs were collected at each stimulation frequency and each was normalized to the amplitude of the initial response at that frequency. Frequency response relationships were determined from the averages of the $\Delta F/F_0$ or PS data for the entire 500 ms pulse train.

Frequency response data for PSs were fit with a 3rd order Butterworth lowpass (dentate synaptic field) or bandpass (CA3 and CA1 synaptic fields) filter with a least squares regression technique using the Levenberg-Marquart method in ProStat (v 5.01, Poly Software International, Pearl River NY) using equations 1 – 3.

$$V_{mean}=A\times\log_{10}(1+fr^{6}) \quad (1)$$

Lowpass:

$$fr=\frac{Hz}{CoF} \quad (2)$$

Bandpass:

$$fr=\left(\frac{Hz}{Cf}-\frac{Cf}{Hz}\right)/Bwf \qquad Bwf=BW/Cf \quad (3)$$

where: V_{mean} is the frequency-dependent gain that was fit to the average PS amplitude during a 500 ms constant frequency or the average PS amplitude at each binned instantaneous frequency during a random frequency stimulus train, Hz is the stimulus frequency, CoF is the cutoff frequency for a low pass filter, Cf is the center frequency for a bandpass filter, BW is the bandwidth of a bandpass filter, and A is a scaling factor that is proportional to the roll off of the filter.

Paired pulse population spike data in figure 5A were fit to equations 4 and 5, which are based on our previously published presynaptic model for the $[Ca^{2+}]_{res}$-dependency of synaptic facilitation (Schiess et al., 2006).

$$R2=F_{Ca}\times P_R 2\times(S-R1)+P_R 2\times\left(1-\frac{R1}{S}\right)\times(1-F_{Ca}) \quad (4)$$

$$F_{Ca} = 1 / \left(1 + \left(\frac{EC \times S}{R1}\right)^{HN}\right) \quad (5)$$

The relationship of the first (*R1*) to the second (*R2*) amplitudes of responses to paired pulses is given in equation 4 where: P_{R2} is the larger, facilitated release probability of *R2*, F_{Ca} is the fraction of vesicles influenced by $[Ca^{2+}]_{res.}$ Based on the assumption that the facilitated pool of vesicles is determined by the interaction of $[Ca^{2+}]_{res}$ with a facilitatory site, we have modeled F_{Ca} to be related to *R1* by a Hill function (equation 5) with: *S* a scaling factor that determines the sensitivity of F_{Ca} to the amplitude of *R1; HN*, the Hill coefficient, which determines the steepness of this relationship; and *EC* the half maximum effective concentration or EC_{50} for $[Ca^{2+}]_{res}$ of the Hill function. Fits to data (Fig 5A) were obtained with the user-defined regression feature of GraphPad Prism (v5.04, GraphPad Software, La Jolla, CA) or Prostat (v 5.01, Poly Software International, Pearl River NY) and fitting parameters are given in Table 1. Comparisons between fits to the model and to a linear regression were made using extra sum-of-squares F test in GraphPad Prism.

Parameters for fits to equations 1, 2, and 3 are given in the figure legends of figures 2, 3, and 7 while parameters for fits to equations 4 and 5 are given in the figure legend of figure 5.

Statistical analysis

Statistical analyses were calculated using either ProStat (v 5.01, Poly Software International, Pearl River NY) or SPSS (Sun Microsystems, Chicago IL). Comparison of fits in figure 5A between the model and a linear regression were calculated with GraphPad Prism (GraphPad Software, La Jolla, CA). Durbin Watson statistics were calculated in SPSS. Significance is indicated with: $P < 0.05$ *, $P < 0.01$ **, $P < 0.005$ ***, $P < 0.001$ ****.

Results

Frequency dependence of $[Ca^{2+}]_{res}$ and fEPSP in hippocampal trisynaptic fields

While analysis of short-term plasticity provides valuable insight into the temporal interaction of homosynaptic inputs occurring at short intervals, a knowledge of the dynamic range of these plastic properties is essential for understanding the physiological characteristics of the transmission of spike trains (Craig and Commins, 2007). In this study, we thus investigated the frequency response of the three synaptic fields in the hippocampal trisynaptic circuit over a physiologically relevant frequency range of 2 to 77 Hz.

Figure 1A shows examples from representative slices of presynaptic $\Delta F/F_0$ and simultaneously recorded field potentials from the beginning and end of approximately 500 ms fixed frequency stimulus trains in the three hippocampal synaptic fields at both 2 Hz and at 30 Hz. It is apparent that there is a summation of $\Delta F/F_0$ at the higher frequency that does not occur at the lower frequency. Furthermore, the amount of multi-pulse plasticity of the population spike (PS), a measure of synaptic gain (Andersen et al., 1980), between the beginning and end of the stimulus train varies among the three synaptic fields. In particular, the PS is considerably reduced by the end the 500 ms fixed frequency stimulus train at both frequencies in the dentate synaptic field while the PS in the CA3 synaptic field exhibits about the same amount of facilitation at the two frequencies and the PS in the CA1 synaptic field shows markedly increased facilitation at the higher frequency.

The PS amplitudes during a train of stimuli will be influenced by both facilitatory and inhibitory factors that are characteristic of specific synapses and interneuronal networks and may respond differently to frequency. Figure 1B shows the time course of the normalized PS

amplitude during the fixed frequency stimulus train at the 8 sampled frequencies between 2 and 77 Hz (respectively 2 to 38 stimulus pulses) in each of the three hippocampal fields. Clearly, the time course of plasticity is highly frequency dependent in this frequency range. Furthermore, while plasticity in the dentate synaptic field is dominated by synaptic depression or network inhibition, the two CA synaptic fields exhibit consistent, but frequency-dependent, facilitation that is most pronounced in the CA1 synaptic field.

An illustrative way to represent the time-dependent data in figure 1 is to plot responses averaged over the whole fixed frequency stimulus train as a function of stimulus frequency. Figure 2 presents summary data for both presynaptic $\Delta F/F_0$ and average postsynaptic PSs as a function of stimulation frequency between 2 and 77 Hz for the three hippocampal synaptic fields. All three presynaptic fields responded with a monotonic increase in the average $\Delta F/F_0$ as a function of stimulation frequency between 2 and 77 Hz.

The frequency response of the three synaptic fields, as determined from the average normalized postsynaptic PS amplitude during the 500 ms fixed frequency pulse train, exhibited characteristics that are unique to each of the three synaptic fields (Fig. 2). In particular, the frequency response of the dentate field is characteristic of a low pass filter while that of the CA fields is characteristic of a bandpass filter. We chose to quantify these filter properties by approximating these relationships as Butterworth filters because of the flat frequency response in the passband that characterizes this type of filter. Thus, we fit the average PS amplitude with a 3rd order Butterworth low pass filter (equations 1 and 2) for the dentate and a 3rd order Butterworth bandpass filter (equations 1 and 3) for the CA3 and CA1 synaptic fields (see Materials and Methods). The frequency response of the dentate synaptic field was markedly different from either of the CA synaptic fields, since the average PS amplitude for the pulse train never showed facilitation, but had a cutoff frequency that attenuated signals above about 18 Hz. Importantly, individual recordings from the dentate synaptic field in the majority of slices (8 out of 12) did exhibit facilitation of the second PS in the train (paired-pulse facilitation or PPF) at frequencies between 10 and 60 Hz; however, the average PS over the entire 500 ms stimulus was still attenuated at frequencies above 18 Hz. In contrast to the dentate, however, both of the CA fields exhibited consistent frequency-dependent facilitation that generated bandpass filter properties with a center frequency of about 12 Hz and a bandwidth of about 21 Hz for CA3 and even narrower bandpass filter properties with a center frequency of about 45 Hz and a bandwidth of about 8 Hz for CA1 (Fig. 2).

In order to test for the possibility that the observed PS frequency responses were unique to the fixed frequency stimulus paradigm used, we measured the frequency response using a random instantaneous frequency paradigm (see Materials and Methods). Stable PS responses were recorded for random instantaneous pulse trains (e.g. Fig 3A) lasting for 10 to 40 s in all three synaptic fields, each in three separate experiments. Figure 3B, shows one representative example from each synaptic field, which clearly indicate that the qualitative features of low pass or bandpass filtering seen in the fixed frequency data are also observed in the random frequency data. Similar results were observed in each of the other two experiments for each synaptic field.

Interneuron involvement in frequency response

In order to assess the contribution of feedback and feedforward inhibitory interneurons to the frequency response properties of each of the three hippocampal synaptic fields, we recorded PS amplitudes before and after a minimum of 5 minutes of bath exposure to the $GABA_A$ receptor antagonist bicuculline (20 μM, Fig 4A). Figure 4B shows the time course of the difference between the PS amplitude in ACSF and that in bicuculline at each time point during the stimulus train at the indicated frequencies between 2 and 77 Hz. In each

synaptic field, the PS amplitudes in bicuculline are generally greater than those in ACSF and the effects are the most marked early in the pulse train and at higher stimulus frequencies. Unexpectedly, in the CA1 synaptic field, at the lower frequencies tested, the bicuculline responses were smaller than those in ACSF.

Since recordings were made in each slice before and after bicuculline application, it was possible to make individual comparisons of the average PS amplitude at each frequency. Figure 4C shows the frequency response for these slices in ACSF (gray) and in 20 μM bicuculline (black) while figure 4D shows the average of differences in PS amplitudes for individual slices. The effect of bicuculline on the frequency response is qualitatively similar in the dentate and CA3 synaptic fields with little effect below about 10 Hz and larger average PS amplitude in bicuculline at higher frequencies. In the CA1 synaptic field there is also an increase in the size of the PS amplitude in bicuculline with respect to that in ACSF at the higher frequencies. This is consistent with feedback and feedforward inhibition having their greatest influence on transmission in the synaptic field at shorter interpulse intervals. In addition, as was apparent in the timecourse data of figure 4B, the average PS amplitude in bicuculline at frequencies below about 30 Hz was unexpectedly smaller in the CA1 synaptic field.

In addition to the contribution of GABAergic feedforward and feedback, particularly to the high frequency roll off of the filter properties, short term synaptic facilitation is likely to contribute to the greater than unity gain in the passband seen in CA3 and CA1. We have previously demonstrated in CA1 that the facilitation of the second of paired pulses as a function of the initial pulse amplitude can be fit accurately with a presynaptic model based on a $[Ca^{2+}]_{res}$-dependent inclusion of a portion of the vesicles in a second facilitated pool that exhibits a higher probability of release (Schiess et al., 2006). In order to test whether this might be an explanation for the passband gain that distinguished the CA fields from the dentate, we assessed differences in short-term plasticity of the afferent synapses among the three synaptic fields by fitting PS amplitudes of the first (R1) vs. the second (R2) of paired pulses generated through an input-output protocol (see Materials and Methods, equations 4 and 5) in the presence of 20 μM bicuculline. Data for each of the three synapses were binned in increments of 0.1 of normalized R1 amplitude and then average values of R2 were plotted as a function of R1 (Fig 5A). Interestingly, there were clear differences in this measure of short term facilitation among these three afferent synapses. In particular, the dentate exhibited a small amount of facilitation over the range of values of R1 (R2 > R1), but the similar fit to the linear and presynaptic (equations 4 and 5) models suggests a minimal non-linear $[Ca^{2+}]_{res}$ dependence of this facilitation. By contrast, PS amplitudes at afferent synapses in both of the CA fields are well fit with the presynaptic model with Schaffer collateral synapses displaying a greater $[Ca^{2+}]_{res}$-dependence of the facilitation process than is exhibited by mossy fiber synapses.

The experiments in figure 4 take advantage of bicuculline block of GABAergic transmission in order to assess the contribution of inhibitory interneurons to the frequency response characteristics of three synaptic fields. An alternative approach to determining the cumulative effect of this network activity is to measure the influence on PS amplitude of the stimulus pulse number at various interpulse intervals. Figure 5B shows the frequency response curves for the difference between average PS amplitudes during the 500 ms pulse train (Figure 2) and either the PS amplitude of the second pulse of the train (equivalent to paired pulse plasticity) or that of the last pulse during the train. Since inhibitory synaptic effects yielding depression or multi-pulse inhibition accumulate during the course of the pulse train, the response to the second pulse tends to be larger than the average while the response to the last pulse tends to be smaller especially at higher frequencies. Interestingly,

these differences are more pronounced in the dentate and CA1 synaptic fields than in the CA3 synaptic field.

Effect of PregS on frequency response properties of three synaptic fields

We have shown previously (Partridge and Valenzuela, 2001) that in the adult hippocampus, the neuroactive steroid, PregS, at concentrations below those necessary to affect postsynaptic receptors, enhances facilitated glutamate release without significantly altering basal release through a mechanism that is downstream from presynaptic $\Delta F/F_0$. Furthermore, we showed frequency-dependent effects of PregS in both the dentate (Thomas et al., 2005) and the CA1 (Partridge and Valenzuela, 2002) synaptic fields. In the present study, we have extended these observations by measuring the effect of PregS on normalized PS and $\Delta F/F_0$ amplitudes at a range of stimulus frequencies in each of the hippocampal synaptic fields.

Figure 6A shows examples from representative slices of presynaptic $\Delta F/F_0$ and simultaneously recorded field potentials from the beginning and end of approximately 500 ms fixed frequency stimulus trains in the three hippocampal synaptic fields at both 2 Hz and at 30 Hz in the presence of 1 μM PregS. Figure 6B shows the average presynaptic $\Delta F/F_0$ as a function of frequency in the three hippocampal synaptic fields in the presence of 1μM PregS. As with the $\Delta F/F_0$ responses in ACSF, the $\Delta F/F_0$ responses in the presence of PregS all increased monotonically with stimulus frequency. Although all three of these sets of data were fit by a linear regression with an $R^2 > 0.9$, there is a tendency in the dentate synaptic field for a frequency-dependent decrease in slope. Figure 6C presents the time course of differences between average PS amplitudes in ACSF and in PregS at each time point during the stimulus train at frequencies between 2 and 77 Hz. Again, there are marked differences in the effect of PregS among the three synaptic fields. In the dentate synaptic field, PregS causes a small increase in PS amplitude, which is maintained at lower frequencies while in both CA synaptic fields, PregS causes large increases in the PS amplitude throughout the duration of the stimulus train that are especially pronounced at higher frequencies.

Our previous results indicated that, in the dentate synaptic field, low concentrations of PregS decrease homosynaptic multi-pulse depression at low frequencies and increase heterosynaptic multi-pulse inhibition at higher frequencies (Thomas et al., 2005) while, in the CA1 synaptic field, low concentrations of PregS enhance the gain of the bandpass filter characteristic of this synaptic field. Figure 7 illustrates the effect of PregS over a physiologically relevant range of frequencies on the filter properties of the three hippocampal synaptic fields. In the dentate synaptic field, 1 μM PregS leads to a small increase in PS amplitude at low frequencies and a small decrease in PS amplitude at higher frequencies (Fig 7A). In the CA3 synaptic field, 1 μM PregS causes an increase in the gain at all frequencies with little change in the bandwidth or center frequency of the passband (Fig 7B). In the CA1 synaptic field, 1μM PregS results in an increase in gain at all frequencies with little change in the bandwith, but a small decrease in the center frequency of the passband. As is apparent in the differences in fits between PregS and ACSF, which are compared in figure 7D, the most dramatic effects of PregS are an enhancement of the ability of the CA3 synaptic field to pass θ frequencies and of the CA1 synaptic field to pass γ frequencies.

Discussion

Summary of findings

In this study, we have extended previous observations of frequency response properties of hippocampal synaptic fields to a broad, physiologically-relevant range of frequencies. While

$[Ca^{2+}]_{res}$ increases monotonically with frequency in the glutamatergic presynaptic terminals of the afferent pathways to the three synaptic fields (Fig 2A), our model suggests that this $[Ca^{2+}]_{res}$ makes a strong contribution to multi-pulse facilitation only in the CA fields (Fig 5A). Within each of the synaptic fields, we would expect that these presynaptic effects could play a role in afferent presynaptic terminals both on principal neurons and onto feedforward inhibitory interneurons. Importantly, in the dentate, GABA interneurons are recruited more strongly than granule cells by the perforant path, which should result in a feedforward inhibition-dependent suppression of granule cell activity (Ewell and Jones, 2010). Interestingly, cumulative inhibitory processes especially in dentate, but also in CA1, dominate at higher frequencies and cause the average PS amplitude over an extended stimulus train to be considerably reduced from the initial PPF (Figs 1B and 5B).

Frequency-dependent GABAergic inhibition through feedback and feedforward interneurons reduces signal amplitude at higher frequencies in all three synaptic fields (Figs 4C & D). Consistent with this observation, the high frequency roll-off, which is characteristic of all of the synaptic fields (Figs 2 & 3), must result from a process downstream from presynaptic $[Ca^{2+}]_{res}$ in the afferent presynaptic terminals, since $[Ca^{2+}]_{res}$ increases monotonically over the extent of the tested frequency range.

The choice of the 500 ms pulse train used in the fixed frequency paradigm of this study was in part dictated by the 2 Hz low frequency extent of the chosen frequency range; however, intracellular recordings of hippocampal place cells exhibit bursts of complex spikes of approximately this duration during an animal's transit of a virtual place field (Harvey et al., 2009). A potential concern in the fixed frequency protocol is that the higher frequencies during some of these pulse trains could induce long-term synaptic plasticity that would affect subsequent PS amplitudes. We attempted to control for this complication by (1) using a half maximum stimulus intensity rather than the maximal intensity often used in LTD and LTP induction protocols, (2) keeping the stimulus frequency below the 100 to 200 Hz range usually necessary for LTP induction (but see (Habib and Dringenberg, 2010)), and (3) applying the stimulus trains in either increasing or decreasing order of fixed frequencies. Importantly, experiments carried out with the random frequency paradigm (Fig. 3) produced frequency responses that were qualitatively similar to those observed with the fixed frequency paradigm in each of the three synaptic fields, indicating that cumulative effects of the 500 ms fixed frequency pulse trains were not uniquely responsible for the observed filter properties. A similar independence of filter properties on stimulus paradigm has been observed in comparing constant-frequency stimulation with a natural stimulus pattern (Kandaswamy et al., 2010).

Hippocampal filter characteristics

The ability of hippocampal synaptic fields to selectively filter specific frequency bands can provide important insight into information processing that is relevant to this brain region. The frequency filtering characteristics of hippocampal synaptic fields that we show here (Figs 2 & 3) are consistent with previously published observations. For instance, slices from the rat dentate gyrus were shown to have low-pass filter characteristics with a cutoff of about 8 Hz (Finnerty et al., 2001). *In vivo* recordings of the rat hippocampus show that transmission into the CA3 synaptic field improves with increasing frequency (Henze et al., 2002), although this study predicts a higher bandpass frequency for the CA3 synaptic field due perhaps to differences between the *in vitro* and *in vivo* preparations including modulatory neurotransmitter systems that are eliminated in the brain slice. When GABAergic transmission is abolished, CA1 pyramidal neurons exhibit high frequency filter properties (Kandaswamy et al., 2010); however network effects in the CA1 synaptic field have been shown to produce an adaptive filtering with a gain of 1.64 at 2 Hz and 2.43 at 40 Hz. Importantly, this bandpass filtering is predicted to be selective for the high frequency

epochs of place cell responses (Klyachko and Stevens, 2006). In general, the dentate synaptic field has been found to exhibit low pass filter characteristics while the CA synaptic fields exhibit bandpass filter characteristics, although to the best of our knowledge we show here the first direct comparison of the filter properties of all three synaptic fields.

Both θ and γ frequency oscillations are important in spatial information encoding in the entorhinal cortex and hippocampus (Chrobak and Buzsaki, 1998; Colgin et al., 2009; Lisman, 2005) and, although average firing rates in these brain region are typically low, complex spikes of several action potentials at γ frequencies (Harris et al., 2001) precess through the θ cycle as an animal traverses a place field (O'Keefe and Recce, 1993). While availability of θ and γ frequency information is important to all of the hippocampal synaptic fields, it is apparent that these signals are transmitted with different effectiveness in each of these synaptic fields. In particular, the dentate synaptic field acts on this information as a low pass filter with little gain while both of the CA fields effectively amplify signals at specific passband frequencies. Importantly, although the low pass filter characteristic of the dentate might be expected to provide a gate keeping function that would prevent entry of γ frequency signals to the trisynaptic circuit, it is not necessary for γ activity generated in the entorhinal cortex transit the dentate synaptic field. First, lower firing rates, within the passband of the dentate synaptic field, can entrain the endogenous γ generators in dentate and CA fields (Csicsvari et al., 2003). Second, the afferent perforant path branches to provide direct input to both the CA3 and CA1 synaptic fields (Yeckel and Berger, 1990) making it possible for higher frequencies to enter the CA synaptic fields after bypassing the dentate altogether.

Contribution of local networks to filter characteristics

Largely GABAergic, but also glutamatergic, interneuronal networks provide the framework for modulation of signals that are relayed through the classic trisynaptic pathway of the hippocampus. The average signal response during a 500 ms stimulus train is the result of time-dependent facilitation and depression processes, which occur at the synaptic input to the principal cell, and excitatory and inhibitory feedforward and feedback effects, which result from local network interactions (Bartos et al., 2011). Frequency-dependent synaptic processes include presynaptic $[Ca^{2+}]_{res}$ accumulation (McGuinness et al., 2010) and pre- and postsynaptic mechanisms downstream from $[Ca^{2+}]_{res}$ (Schiess et al., 2006). Our modeling of the data in figure 5A suggest that these downstream $[Ca^{2+}]_{res}$-dependent facilitatory processes make a more significant contribution in the CA fields than in the dentate. In the majority of measurements presented here, the actions of the interneuronal networks certainly contribute to the frequency responses that we measured. In the experiments shown in figure 4, we assessed the contributions of GABAergic interneuronal networks by comparing frequency response characteristics of the three synaptic fields before and after bath application of bicuculline. In marked contrast to the minimal $[Ca^{2+}]_{res}$-dependent presynaptic effects seen in the dentate, the frequency response of this synaptic field is significantly molded by contributions from GABAergic interneurons.

Over the range of frequencies studied here, it is generally expected that network effects will be more influential at short interpulse intervals while, at longer intervals, presynaptic mechanisms in the afferent terminals onto the principal cell will predominate (Steffensen et al., 2006; Thomas et al., 2005). Our results in CA3 and dentate (Fig 4C & D) are consistent with this interpretation, since bicuculline has little effect on PS amplitude at low frequencies while at higher frequencies, removing GABAergic network inhibition tends to increase PS amplitude.

A previous study of the Schaffer collateral to CA1 synaptic response to steady state frequencies in the presence of picrotoxin found synaptic depression at frequencies between 2

and 10 Hz (Sun et al., 2005). Interestingly, we found that bicuculline eliminated the facilitation of the average PS response that we observed over this frequency range in ACSF (Fig 4C). A possible explanation for the decrease in the multi-pulse facilitation that we observed in CA1 when $GABA_A$ transmission was blocked may lie in the observation that feedforward GABAergic interneurons in CA1 exhibit stimulus intensity-dependent paired pulse depression of their unitary IPSPs onto pyramidal neurons (Bertrand and Lacaille, 2001). Thus, in ACSF, the second and subsequent PSs would be relatively larger because they are affected by less feedforward inhibition. This effect could be especially significant in CA1 because of the very prominent $[Ca^{2+}]_{res}$-dependent facilitation of glutamate release (Fig 5A).

$[Ca^{2+}]_{res}$-dependent contributions to filtering

It is well established that presynaptic $[Ca^{2+}]_{res}$ plays a crucial role in facilitation at individual synaptic terminals (e.g. (Dittman et al., 2000)). However, the frequency dependence of PS amplitude (Figs 2 & 3) represents the throughput of the synaptic field from the presynaptic action potential to the postsynaptic electrical response of the principal neuron and includes feedback and feedforward effects of local interneurons. In all three synaptic fields, the PS amplitude falls off at higher frequencies. On the other hand, the frequency dependence of the $\Delta F/F_0$ signal (Fig 2A) represents only the presynaptic $[Ca^{2+}]_{res}$ response to the presynaptic action potential and, in all three synaptic fields, this response rises monotonically with increasing frequency over the measured range. Importantly, control experiments (see Materials and Methods) with ionotropic receptor blockers and TTX indicate that the $\Delta F/F_0$ signal is localized to the presynaptic axon terminals and does not include significant contributions from postsynaptic principal cells or interneurons. Thus, differences between the frequency-dependent properties of the PS and $\Delta F/F_0$ responses are indicative of events downstream from presynaptic $[Ca^{2+}]_{res}$ in the afferent presynaptic terminals of each synaptic field. These downstream effects include vesicle release processes in the presynaptic terminals, feedback and feedforward effects onto the principal cells, and frequency-dependent effects of the postsynaptic receptors. This interpretation suggests that, in all three synaptic fields, the most prominent effect of mechanisms downstream from presynaptic $[Ca^{2+}]_{res}$ is the high frequency roll off that contributes to the low pass filter in the dentate synaptic field and the high frequency stopband of the bandpass filter in the CA synaptic fields. This is consistent with observations from modeling experiments that predict a high frequency cutoff characteristic of dendritic dipoles on local field potentials (Linden et al., 2010).

The presynaptic components of short-term synaptic plasticity have been successfully modeled with a $[Ca^{2+}]_{res}$-dependent facilitatory process that is antagonized in a frequency- and time-dependent manner by cumulative synaptic depression (Dittman et al., 2000; Schiess et al., 2006). We used a similar model to fit input-output data from the three synaptic fields and found rather distinct properties for each field (Fig 5A). Notably, we found a more dominant $[Ca^{2+}]_{res}$-dependent facilitatory process in the synaptic inputs to the CA fields than in the input to the dentate. In addition, by comparing the PS amplitude of either the second pulse (paired-pulse plasticity) or the last pulse in a 500 ms train with the average for the whole train (Fig 5B), our results give an indication of the importance of the $[Ca^{2+}]_{res}$-dependent facilitatory process of this model in the three synaptic fields. In the dentate and CA1 synaptic fields at higher frequencies, paired-pulse responses are greatly facilitated when compared with the average response over 500 ms. This is consistent with an important contribution from the summation of synaptic depression and/or network inhibition at short interpulse intervals. Interestingly, the CA3 synaptic field does not show this pronounced effect and suggests less of a cumulative contribution from depression and/or inhibition.

Effect of PregS on filter characteristics

Among the documented cognitive and memory enhancing effects of sulfated neurosteroids, is the observation that they can improve spatial memory (Johnson et al., 2000) and thus it is appropriate to ask how they affect hippocampal signal processing. We have shown previously that μM or lower concentrations of PregS have an enhancing effect on facilitated glutamate release with very little effect on basal release in slices from mature rats (Partridge and Valenzuela, 2001; Schiess et al., 2006; Thomas et al., 2005). The data presented here (Fig 7) generally confirm these findings and extend the observations to all three hippocampal synaptic fields, over the physiologically relevant frequency range of 2 Hz to 77 Hz, and to the effect of PregS on presynaptic $[Ca^{2+}]_{res}$ (Fig 6B). In particular, we observed previously that, in the dentate synaptic field, PregS caused an approximately 5% increase in multi-pulse inhibition of fEPSPs after 5 pulses at 50 Hz, and an approximately 10% decrease in multi-pulse depression of fEPSPs after 10 pulses at 14 Hz (Thomas et al., 2005). Figure 7A shows that, when the PS amplitude is averaged over a longer pulse train, there was a similar trend, although the differences are no longer significant. In another study, we observed that, in the CA1 synaptic field, PregS caused a frequency-dependent enhancement of the intracellularly recorded PSP at the end of a 300 ms stimulus train with peak enhancement occurring at 21 Hz (Partridge and Valenzuela, 2002). Figure 7C shows a similar phenomenon with an enhancement of the bandpass filter characteristics of the average PS during a longer 500 ms pulse train. Differences between the fits to frequency response data in ACSF and PregS (Fig 7D) emphasize the marked differences in the effect that this neuroactive steroid has on signal transmission in the three synaptic fields.

Endogenous neurosteroids can play important roles in cognitive functions and we show here that one mechanism for this could to be their effect on filtering of information by the hippocampal synaptic fields. Our observations indicate that θ frequencies are not only easily transmitted by all three hippocampal synaptic fields, but PregS enhances transmission of these frequencies in both CA synaptic fields. It is well established that precession of single unit activity through the θ cycle is a central feature of encoding of place fields (O'Keefe and Recce, 1993) and the enhancement by PregS of gain in the θ frequency range in the CA synaptic fields may help explain the improved spatial navigation of animals with increased endogenous levels of sulphated neurosteroids (Johnson et al., 2000). We predict that firing frequencies in the γ range would be effectively eliminated by filtering of the perforant path inputs to the dentate synaptic field, but direct perforant path input to the CA fields could bypass this low pass filter. Our observations predict that signals in the γ frequency range would be easily transmitted through the CA1 synaptic field and this transmission would be additionally enhanced by PregS. The importance of a PregS-dependent increased gain in the γ frequency range is less obvious since, although γ generators have been identified in the dentate gyrus and the CA regions and coherence between γ frequency currents may entrain firing of place cells in different locations (Csicsvari et al., 2003), hippocampal neurons do not exhibit sustained firing at γ frequencies. Importantly, however, hippocampal principal neurons exhibit complex spikes with significant power in the γ frequency band (Harvey et al., 2009; Yue and Yaari, 2004) and this firing has implications for information processing (Goonawardena et al., 2011); consequently the enhancement by PregS of gain in the CA1 synaptic field may contribute to the cognitive effects of this neuroactive steroid. Thus, while it is clear that the basal firing rate of hippocampal principal cells is typically less than 10 Hz, the effects of PregS that we have described here are likely to be especially significant in transmission of activity-dependent firing at considerably higher frequencies.

Acknowledgments

This work was supported by MH07387 from the National Institutes of Health. The authors thank Fernando Valenzuela, Marvin Diaz and Russell Morton for critical reading of this manuscript

References

Ahmed OJ, Mehta MR. The hippocampal rate code: anatomy, physiology and theory. Trends Neurosci. 2009; 32(6):329–38. [PubMed: 19406485]

Andersen, P. Organization of hippocampal neurons and their interconnections. In: Pribram, RIK., editor. The Hippocampus Volume I: Structure and Development. New York: Plenum; 1975. p. 155-175.

Andersen P, Sundberg SH, Sveen O, Swann JW, Wigstrom H. Possible mechanisms for long-lasting potentiation of synaptic transmission in hippocampal slices from guinea-pigs. J Physiol. 1980; 302:463–82. [PubMed: 7411464]

Andersson R, Lindskog M, Fisahn A. Histamine H3 receptor activation decreases kainate-induced hippocampal gamma oscillations in vitro by action potential desynchronization in pyramidal neurons. J Physiol. 2010; 588(Pt 8):1241–9. [PubMed: 20156850]

Atluri PP, Regehr WG. Determinants of the time course of facilitation at the granule cell to Purkinje cell synapse. J Neurosci. 1996; 16(18):5661–71. [PubMed: 8795622]

Bartos M, Alle H, Vida I. Role of microcircuit structure and input integration in hippocampal interneuron recruitment and plasticity. Neuropharmacology. 2011; 60(5):730–9. [PubMed: 21195097]

Bertrand S, Lacaille JC. Unitary synaptic currents between lacunosum-moleculare interneurones and pyramidal cells in rat hippocampus. J Physiol. 2001; 532(Pt 2):369–84. [PubMed: 11306657]

Bliss TV, Collingridge GL. A synaptic model of memory: long-term potentiation in the hippocampus. Nature. 1993; 361(6407):31–9. [PubMed: 8421494]

Chen L, Cai W, Zhou R, Furuya K, Sokabe M. Modulatory metaplasticity induced by pregnenolone sulfate in the rat hippocampus: a leftward shift in LTP/LTD-frequency curve. Hippocampus. 2010; 20(4):499–512. [PubMed: 19475651]

Chrobak JJ, Buzsaki G. Gamma oscillations in the entorhinal cortex of the freely behaving rat. J Neurosci. 1998; 18(1):388–98. [PubMed: 9412515]

Colgin LL, Denninger T, Fyhn M, Hafting T, Bonnevie T, Jensen O, Moser MB, Moser EI. Frequency of gamma oscillations routes flow of information in the hippocampus. Nature. 2009; 462(7271): 353–7. [PubMed: 19924214]

Craig S, Commins S. Plastic and metaplastic changes in the CA1 and subicular projections to the entorhinal cortex. Brain Res. 2007; 1147:124–39. [PubMed: 17368431]

Csicsvari J, Jamieson B, Wise KD, Buzsaki G. Mechanisms of gamma oscillations in the hippocampus of the behaving rat. Neuron. 2003; 37(2):311–22. [PubMed: 12546825]

Deng PY, Klyachko VA. The diverse functions of short-term plasticity components in synaptic computations. Communicative & integrative biology. 2011; 4(5):543–8. [PubMed: 22046457]

Dittman JS, Kreitzer AC, Regehr WG. Interplay between facilitation, depression, and residual calcium at three presynaptic terminals. J Neurosci. 2000; 20(4):1374–85. [PubMed: 10662828]

Ewell LA, Jones MV. Frequency-tuned distribution of inhibition in the dentate gyrus. J Neurosci. 2010; 30(38):12597–607. [PubMed: 20861366]

Finnerty GT, Whittington MA, Jefferys JG. Altered dentate filtering during the transition to seizure in the rat tetanus toxin model of epilepsy. J Neurophysiol. 2001; 86(6):2748–53. [PubMed: 11731534]

Freund TF, Buzsaki G. Interneurons of the hippocampus. Hippocampus. 1996; 6(4):347–470. [PubMed: 8915675]

Gibbs TT, Russek SJ, Farb DH. Sulfated steroids as endogenous neuromodulators. Pharmacol Biochem Behav. 2006; 84(4):555–67. [PubMed: 17023038]

Goonawardena AV, Riedel G, Hampson RE. Cannabinoids alter spontaneous firing, bursting, and cell synchrony of hippocampal principal cells. Hippocampus. 2011; 21(5):520–31. [PubMed: 20101600]

Griguoli M, Cherubini E. Regulation of hippocampal inhibitory circuits by nicotinic acetylcholine receptors. The Journal of physiology. 2011

Gulyas AI, Szabo GG, Ulbert I, Holderith N, Monyer H, Erdelyi F, Szabo G, Freund TF, Hajos N. Parvalbumin-containing fast-spiking basket cells generate the field potential oscillations induced

by cholinergic receptor activation in the hippocampus. J Neurosci. 2010; 30(45):15134–45. [PubMed: 21068319]

Habib D, Dringenberg HC. Low-frequency-induced synaptic potentiation: a paradigm shift in the field of memory-related plasticity mechanisms? Hippocampus. 2010; 20(1):29–35. [PubMed: 19405136]

Harris KD, Hirase H, Leinekugel X, Henze DA, Buzsaki G. Temporal interaction between single spikes and complex spike bursts in hippocampal pyramidal cells. Neuron. 2001; 32(1):141–9. [PubMed: 11604145]

Harvey CD, Collman F, Dombeck DA, Tank DW. Intracellular dynamics of hippocampal place cells during virtual navigation. Nature. 2009; 461(7266):941–6. [PubMed: 19829374]

Henze DA, Wittner L, Buzsaki G. Single granule cells reliably discharge targets in the hippocampal CA3 network in vivo. Nat Neurosci. 2002; 5(8):790–5. [PubMed: 12118256]

Holderith N, Nemeth B, Papp OI, Veres JM, Nagy GA, Hajos N. Cannabinoids attenuate hippocampal gamma oscillations by suppressing excitatory synaptic input onto CA3 pyramidal neurons and fast spiking basket cells. The Journal of physiology. 2011

Johnson DA, Wu T, Li P, Maher TJ. The effect of steroid sulfatase inhibition on learning and spatial memory. Brain Res. 2000; 865(2):286–90. [PubMed: 10821934]

Kandaswamy U, Deng PY, Stevens CF, Klyachko VA. The role of presynaptic dynamics in processing of natural spike trains in hippocampal synapses. J Neurosci. 2010; 30(47):15904–14. [PubMed: 21106829]

Klyachko VA, Stevens CF. Excitatory and feed-forward inhibitory hippocampal synapses work synergistically as an adaptive filter of natural spike trains. PLoS Biol. 2006; 4(7):e207. [PubMed: 16774451]

Kobayashi T, Washiyama K, Ikeda K. Pregnenolone sulfate potentiates the inwardly rectifying K channel Kir2.3. PLoS One. 2009; 4(7):e6311. [PubMed: 19621089]

Linden H, Pettersen KH, Einevoll GT. Intrinsic dendritic filtering gives low-pass power spectra of local field potentials. J Comput Neurosci. 2010; 29(3):423–44. [PubMed: 20502952]

Lisman J. The theta/gamma discrete phase code occuring during the hippocampal phase precession may be a more general brain coding scheme. Hippocampus. 2005; 15(7):913–22. [PubMed: 16161035]

McGuinness L, Taylor C, Taylor RD, Yau C, Langenhan T, Hart ML, Christian H, Tynan PW, Donnelly P, Emptage NJ. Presynaptic NMDARs in the hippocampus facilitate transmitter release at theta frequency. Neuron. 2010; 68(6):1109–27. [PubMed: 21172613]

Mongillo G, Barak O, Tsodyks M. Synaptic theory of working memory. Science. 2008; 319(5869): 1543–6. [PubMed: 18339943]

O'Keefe J, Recce ML. Phase relationship between hippocampal place units and the EEG theta rhythm. Hippocampus. 1993; 3(3):317–30. [PubMed: 8353611]

Okun M, Naim A, Lampl I. The subthreshold relation between cortical local field potential and neuronal firing unveiled by intracellular recordings in awake rats. J Neurosci. 2010; 30(12):4440–8. [PubMed: 20335480]

Partridge LD, Valenzuela CF. Neurosteroid-induced enhancement of glutamate transmission in rat hippocampal slices. Neurosci Lett. 2001; 301(2):103–6. [PubMed: 11248433]

Partridge LD, Valenzuela CF. Neurosteroids enhance bandpass filter characteristics of the rat Schaffer collateral-to-CA1 synapse. Neurosci Lett. 2002; 326(1):1–4. [PubMed: 12052524]

Reddy DS. Neurosteroids: endogenous role in the human brain and therapeutic potentials. Progress in brain research. 2010; 186:113–37. [PubMed: 21094889]

Regehr WG, Atluri PP. Calcium transients in cerebellar granule cell presynaptic terminals. Biophys J. 1995; 68(5):2156–70. [PubMed: 7612860]

Regehr WG, Delaney KR, Tank DW. The role of presynaptic calcium in short-term enhancement at the hippocampal mossy fiber synapse. J Neurosci. 1994; 14(2):523–37. [PubMed: 8301352]

Schiess AR, Scullin CS, Partridge LD. Neurosteroid-induced enhancement of short-term facilitation involves a component downstream from presynaptic calcium in hippocampal slices. J Physiol. 2006; 576(Pt 3):833–47. [PubMed: 16931546]

Scullin CS, Partridge LD. Contributions of SERCA pump and ryanodine-sensitive stores to presynaptic residual Ca2+ Cell calcium. 2010; 47(4):326–38. [PubMed: 20153896]

Speed HE, Dobrunz LE. Developmental changes in short-term facilitation are opposite at temporoammonic synapses compared to Schaffer collateral synapses onto CA1 pyramidal cells. Hippocampus. 2009; 19(2):187–204. [PubMed: 18777561]

Steffensen SC, Jones MD, Hales K, Allison DW. Dehydroepiandrosterone sulfate and estrone sulfate reduce GABA-recurrent inhibition in the hippocampus via muscarinic acetylcholine receptors. Hippocampus. 2006; 16(12):1080–90. [PubMed: 17024678]

Sun HY, Lyons SA, Dobrunz LE. Mechanisms of target-cell specific short-term plasticity at Schaffer collateral synapses onto interneurones versus pyramidal cells in juvenile rats. J Physiol. 2005; 568(Pt 3):815–40. [PubMed: 16109728]

Thomas MJ, Mameli M, Carta M, Valenzuela CF, Li PK, Partridge LD. Neurosteroid paradoxical enhancement of paired-pulse inhibition through paired-pulse facilitation of inhibitory circuits in dentate granule cells. Neuropharmacology. 2005; 48(4):584–96. [PubMed: 15755486]

Traub RD, Pais I, Bibbig A, Lebeau FE, Buhl EH, Garner H, Monyer H, Whittington MA. Transient depression of excitatory synapses on interneurons contributes to epileptiform bursts during gamma oscillations in the mouse hippocampal slice. J Neurophysiol. 2005; 94(2):1225–35. [PubMed: 15728773]

Valenzuela CF, Partridge LD, Mameli M, Meyer DA. Modulation of glutamatergic transmission by sulfated steroids: role in fetal alcohol spectrum disorder. Brain Res Rev. 2008; 57(2):506–19. [PubMed: 17597219]

Vallee M, Mayo W, Darnaudery M, Corpechot C, Young J, Koehl M, Le Moal M, Baulieu EE, Robel P, Simon H. Neurosteroids: deficient cognitive performance in aged rats depends on low pregnenolone sulfate levels in the hippocampus. Proceedings of the National Academy of Sciences of the United States of America. 1997; 94(26):14865–70. [PubMed: 9405705]

Whittingstall K, Logothetis NK. Frequency-band coupling in surface EEG reflects spiking activity in monkey visual cortex. Neuron. 2009; 64(2):281–9. [PubMed: 19874794]

Yeckel MF, Berger TW. Feedforward excitation of the hippocampus by afferents from the entorhinal cortex: redefinition of the role of the trisynaptic pathway. Proc Natl Acad Sci U S A. 1990; 87(15): 5832–6. [PubMed: 2377621]

Yue C, Yaari Y. KCNQ/M channels control spike afterdepolarization and burst generation in hippocampal neurons. J Neurosci. 2004; 24(19):4614–24. [PubMed: 15140933]

Zheng P. Neuroactive steroid regulation of neurotransmitter release in the CNS: action, mechanism and possible significance. Progress in neurobiology. 2009; 89(2):134–52. [PubMed: 19595736]

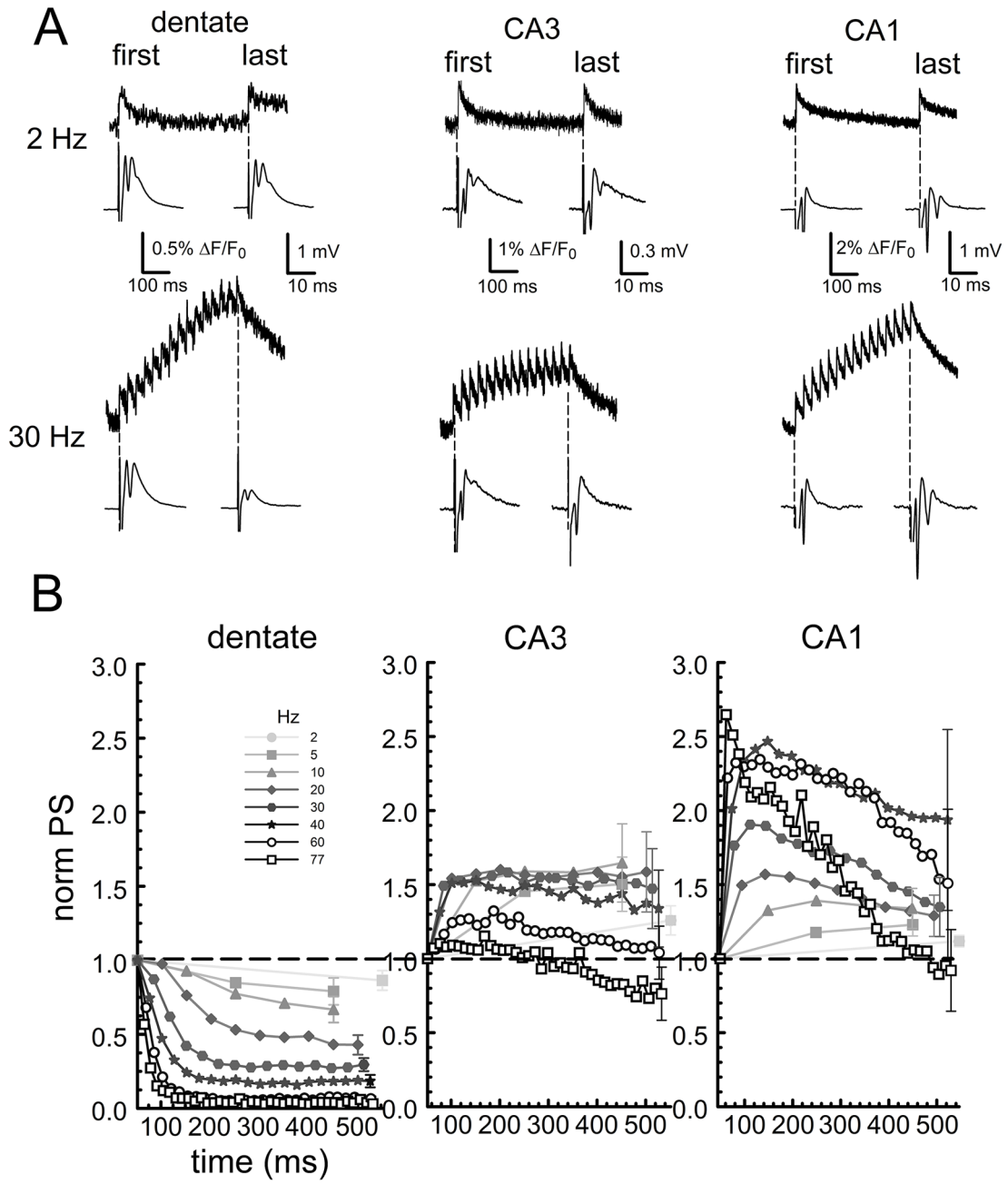

Figure 1.

Presynaptic $\Delta F/F_0$ and postsynaptic fEPSPs during fixed frequency 500 ms stimulus trains in three hippocampal synaptic fields. **A**. Representative traces at 2 Hz top and 30 Hz bottom. fEPSP traces, at expanded time scales, are shown for the first and last pulse at each frequency. **B**. Time course of normalized PS amplitude at 8 frequencies between 2 Hz and 77 Hz (see inset). For clarity, standard errors of the mean are shown for only the last time point. (dentate, n = 11; CA3, n = 17; CA1, n = 15.)

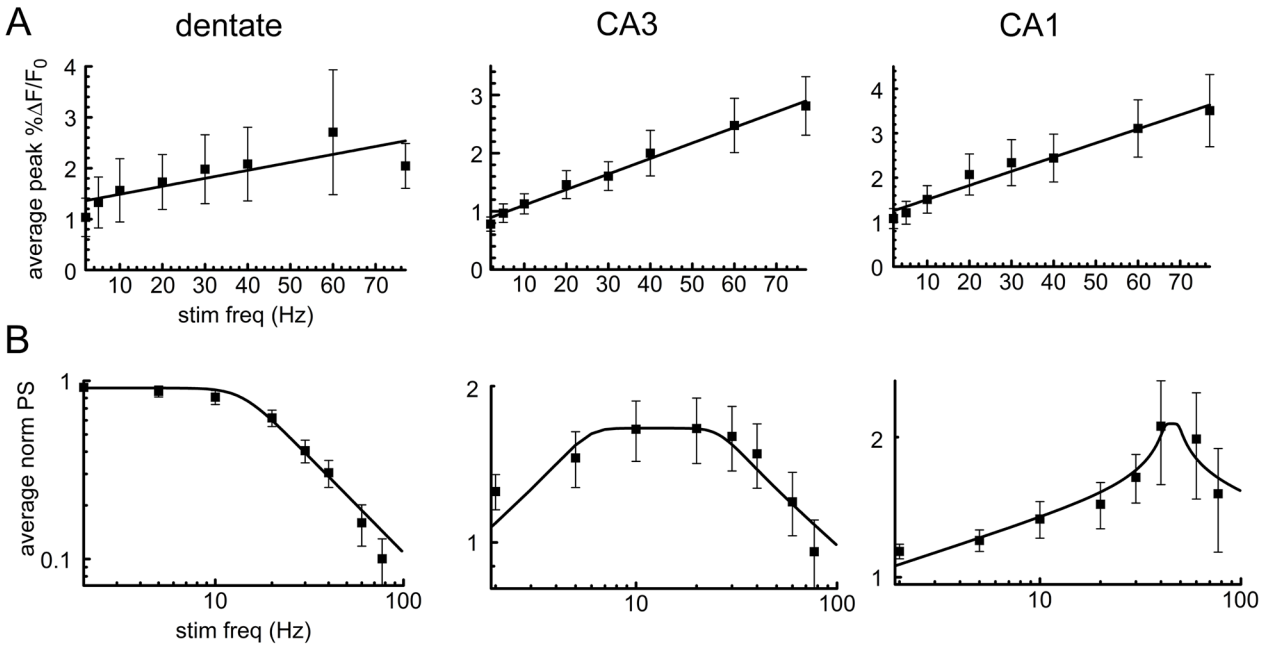

Figure 2.

Frequency response relationships of each of the three hippocampal synaptic fields measured with fixed frequency stimulus trains. $\Delta F/F_0$ (**A**) and average PS amplitude (**B**) are shown for each of the three hippocampal synaptic fields. $\Delta F/F_0$ data are fit with a least squares linear regression ($\Delta F/F_0 = a \times Hz + b$: dentate a = 0.016, b = 1.330, $R^2 = 0.674$, n = 7; CA3 a = 0.027, b = 0.840, $R^2 = 0.990$, n = 17; CA1 a = 0.032, b = 1.191, $R^2 = 0.970$, n = 11). PS data are fit with a least squares regression to a low pass (equations 1 and 2, dentate) or bandpass (equations 1 and 3, CA3 and CA1) 3rd order Butterworth filter (see Methods). Dentate COF = 13.781 Hz, A = 0.179, $R^2 = 0.995$, n = 9; CA3 CF = 12.292 Hz, BW = 21.272 Hz, A = 0.056, $R^2 = 0.941$, n = 18; CA1 CF = 45.304 Hz, BW = 7.650 Hz, A = 0.024, $R^2 = 0.960$, n = 16.

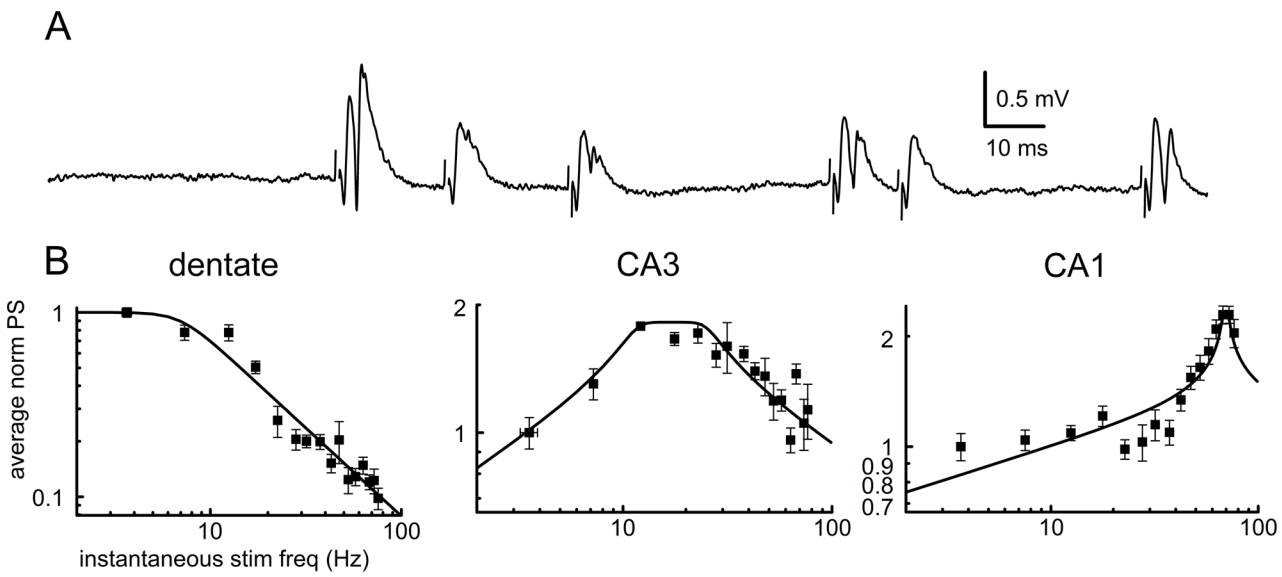

Figure 3.

Frequency response relationships of each of the three hippocampal synaptic fields measured with random frequency stimulus trains. **A**. Exemplar portion of an 11 s PS record from the dentate. Note that PS amplitudes are larger following long intervals (low instantaneous frequency) than after short intervals (high instantaneous frequency). **B**. Data from the whole 11 s record from the dentate or similar records from the CA fields are fit with a least squares regression to a low pass (dentate, equations 1 and 2) or bandpass (CA3 and CA1, equations 1 and 3) 3rd order Butterworth filter (see Methods). Dentate: example, COF = 6.975, A= 0.159, R^2 = 0.947; average for 3 slices COF = 9.748 ± 3.573 Hz. CA3: example, CF = 17.729 Hz, BW = 14.613 Hz, A = 0.0567, R^2 = 0.811; average for 3 slices CF = 32.195 ± 17.383 Hz, BW = 21.839± 9.813 Hz; CA1: example, CF = 69.645 Hz, BW = 4.829 Hz, A = 0.0299, R^2 = 0.865; average for 3 slices CF = 62.186 ± 5.108 Hz, BW = 11.272 ± 3.591 Hz.

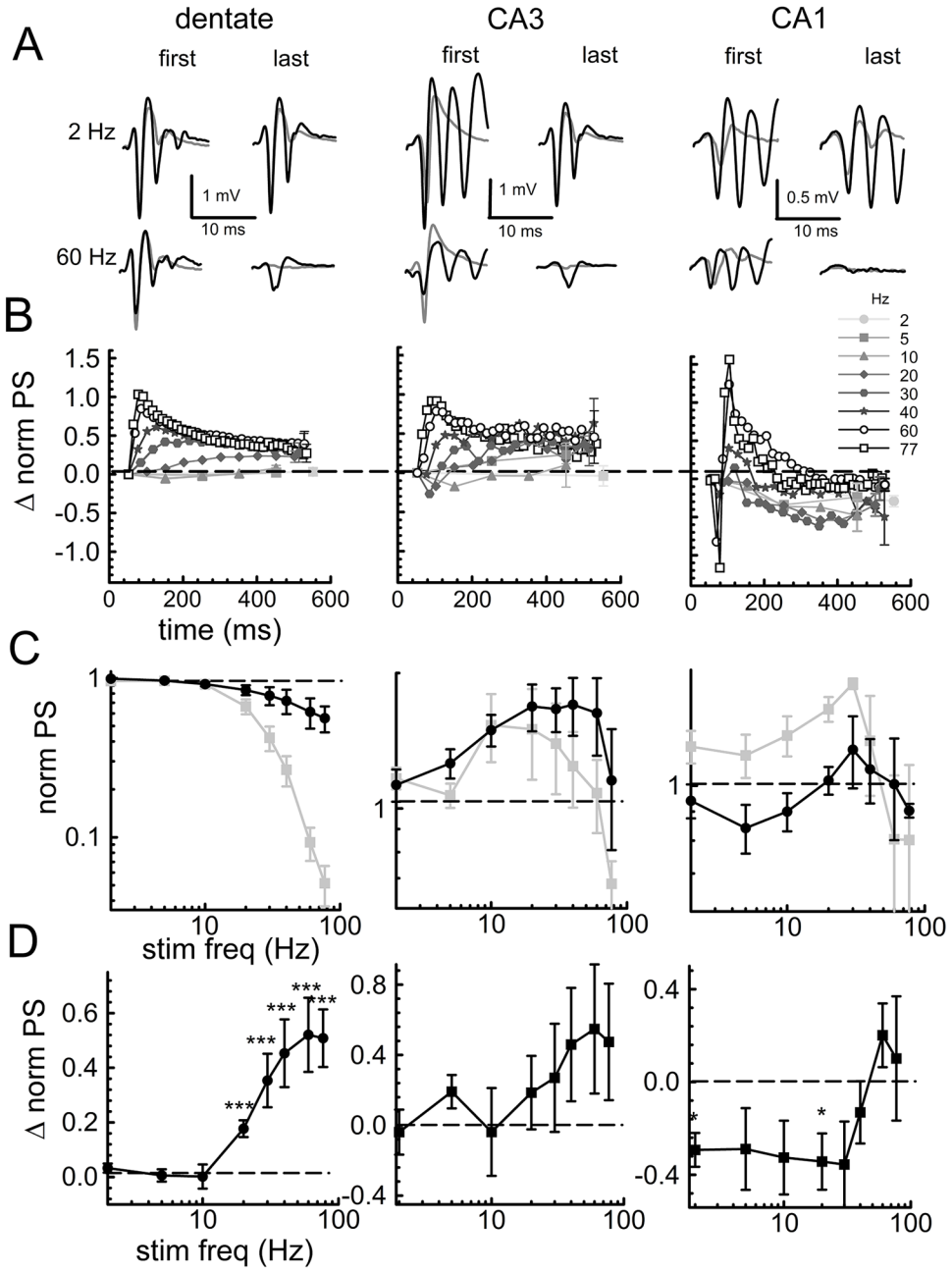

Figure 4.

Contribution of network inhibition to PS frequency response. **A**. First and last representative fEPSP traces during a 500 ms stimulus at 2 Hz (top) and 60 Hz (bottom) recorded in ACSF (gray) and in the same slice in 20 μM bicuculline (black). Note: As expected, bicuculline caused multiple PSs and measurements of PS amplitude were restricted to the first one following the stimulus artifact. **B**. Time course of the difference (bicuculline – ACSF) in individual slices between initial PS amplitude in ACSF and in 20 μM bicuculline at frequencies between 2 and 77 Hz (see inset). (dentate, n = 12; CA3, n = 12; CA1, n = 8.) **C.** Frequency response curves for PS amplitude in individual slices ACSF (gray) and bicuculline (black) during a 500 ms pulse train. D. Frequency dependency of differences in

normalized PS amplitude for individual slices (bicuculline – ACSF). (One-way ANOVA with posthoc *t*-test against population mean of 0. Dentate: $F_{(6,35)} = 6.21$, $P = <0.0005$, n = 12; CA3: $F_{(7,40)} = 0.71$, $P = 0.66$, n = 12; CA1: $F_{(7,24)} = 1.72$, $P = 0.15$, n = 8).

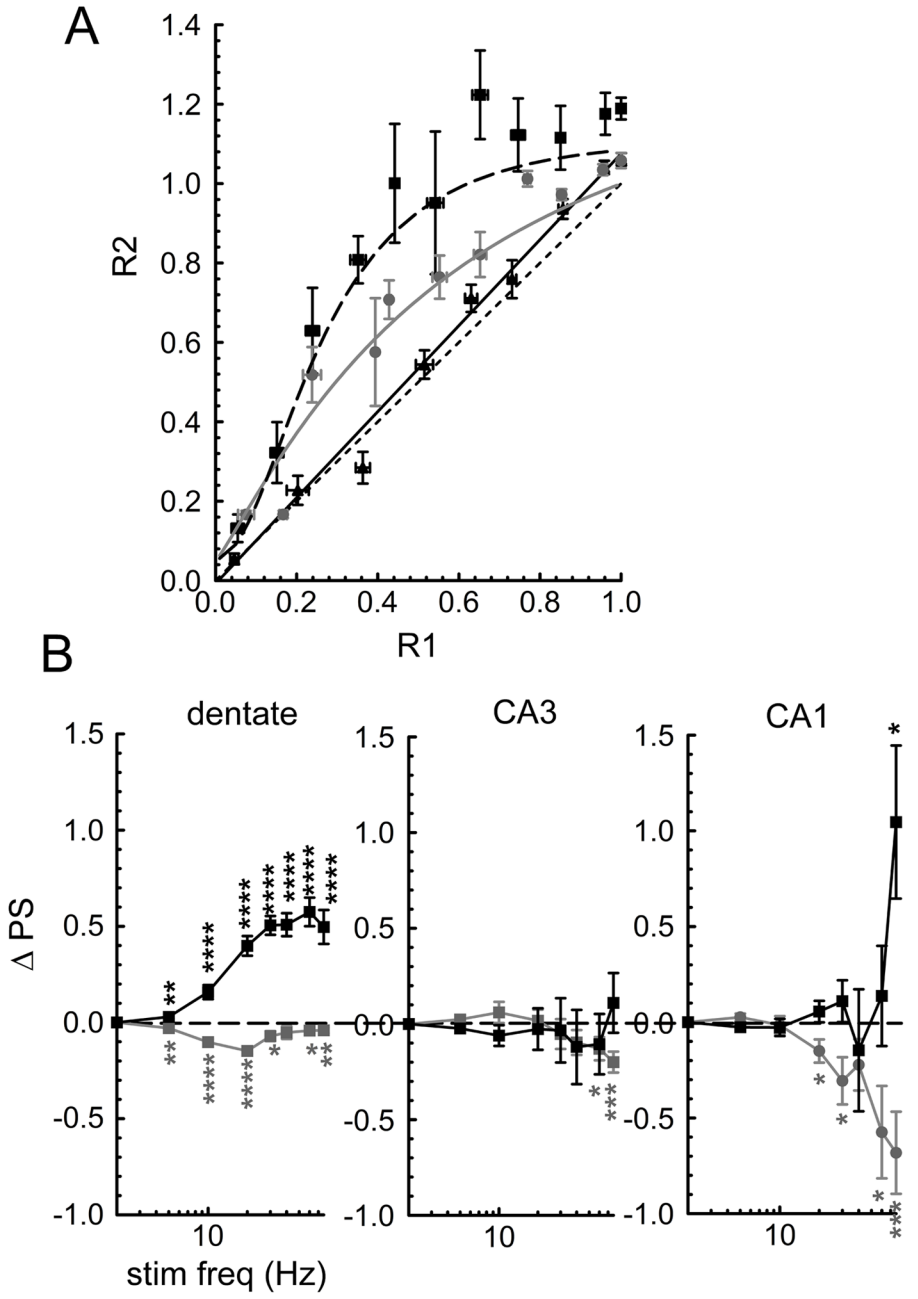

Figure 5.

Effect of cumulative depression on PS frequency response. **A**. R1 vs. R2 PS amplitudes from input-output analyses at 50 ms interpulse interval in 20 μM bicuculline normalized to maximum value of R1 for each slice. Data are grouped in bins of 0.1 × R1 and average values ± s.e.m. are shown; however fits are to un-binned data. For the data from the dentate, there was no difference between the fits with the linear model (black solid line ▲, slope = 1.08 ± 0.0244, intercept = −0.00750 ± 0.01835) and the presynaptic model (comparison of fits: $F_{(3,69)} = 0.2522$, $P = 0.8589$, Durbin Watson statistic = 2.236 indicates a lack of serial correlation, n = 10 slices). Data from CA3 were better fit with the presynaptic model (equations 4 and 5, table 1, gray solid line ●) than a linear model (comparison of fits $F_{(3,61)}$

= 6.290, $P < 0.001$, Durbin Watson statistic = 1.578 indicates a weak serial correlation suggesting linearity, n = 9 slices). Data from CA1 were better fit with the presynaptic model (equations 4 and 5, table 1, black dashed line ■) than with a linear model (comparison of fits: $F_{(3,55)} = 11.58$, $P < 0.0001$, Durbin Watson statistic = 0.860 indicates a strong serial correlation, n = 8 slices). (Black dotted line indicates unity slope.) **B**. Frequency response curves for the difference between either the first PS in the train (PPF) (black) or the last PS in the train (gray) and the average PS amplitude during a 500 ms pulse train. (One-way ANOVA with posthoc *t*-test against population mean of 0. Dentate: PPF - average, $F_{(7,79)} = 18.17$ $P < .00001$; end – average, $F_{(7,79)} = 6.01$, $P < 0.00001$, n = 11; CA3, PPF – average, $F_{(7,125)} = 0.29$, $P=0.96$, end – average $F_{(7,125)} = 2.40$, $P < 0.05$, n = 17; CA1: PPF – average, $F_{(7,108)} = 3.34$, $P < 0.005$, n = 15).

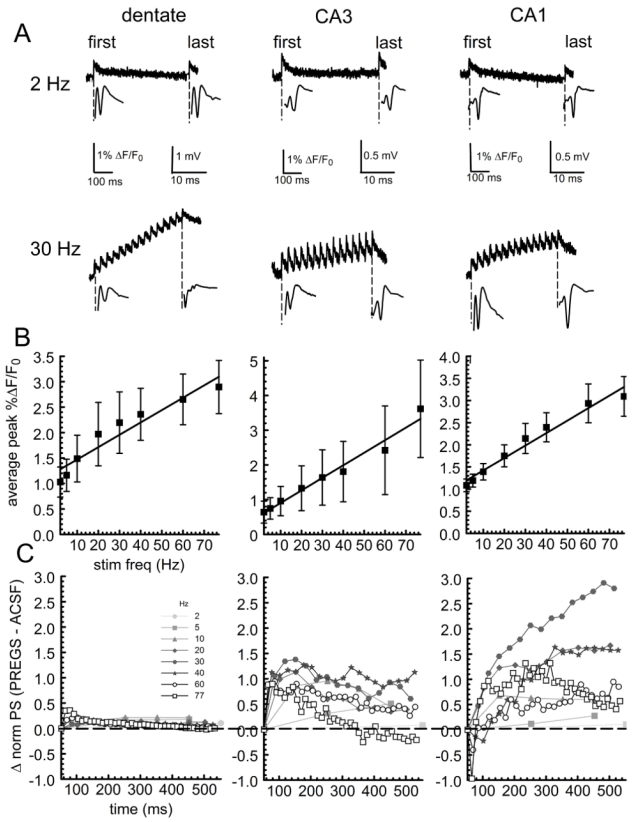

Figure 6.

PS and $\Delta F/F_0$ response for three hippocampal synaptic fields in PregS. **A**. Representative traces at 2 Hz top and 30 Hz bottom in 1 μM PregS. PS traces at faster sweeps are shown for the first and last pulse at each frequency. **B.** $\Delta F/F_0$ data are fit with a least squares linear regression ($\Delta F/F_0 = a \times Hz + b$: dentate, a = 0.024, b = 1.23, $R^2 = 0.913$, n = 7; CA3, a = 0.036, b = 0.542, $R^2 = 0.970$, n = 6, CA1, a = 0.028, b = 1.139, $R^2 = 0.970$, n = 13). **C**. Time course of the difference between average PS amplitude in ACSF and the average PS amplitude in 1μM PregS at frequencies between 2 and 77 Hz (see inset).

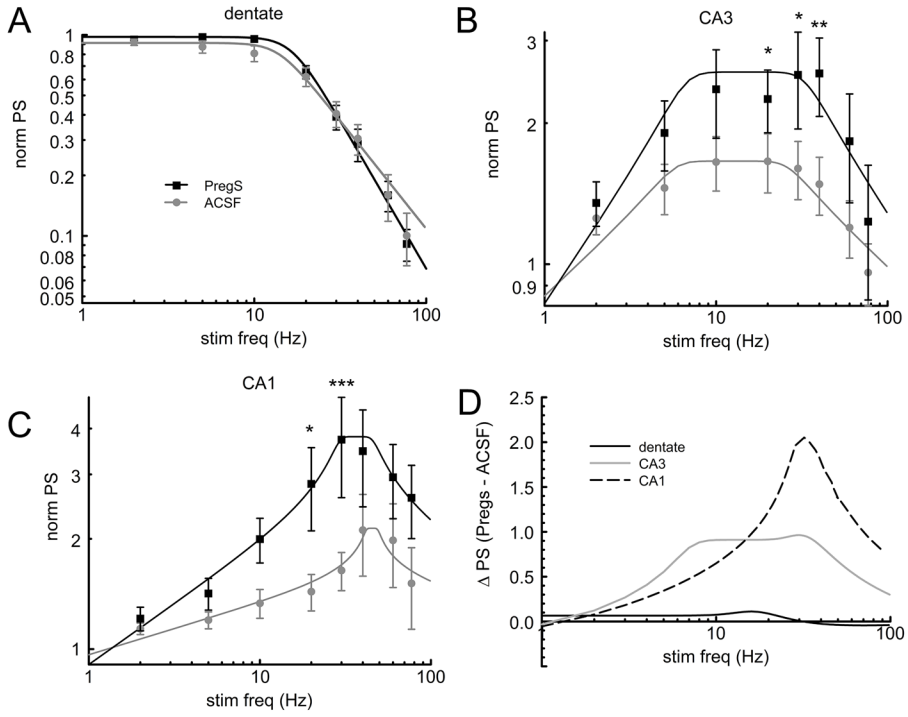

Figure 7.

Comparison of frequency responses in ACSF (gray ● and PregS black ■). PS data are fit with a least squares regression to a low pass (**A**, dentate) or bandpass (**B**, CA3 and **C**, CA1) 3rd order Butterworth filter (see Methods). Parameters for ACSF fits are given in figure 2. PregS fits: dentate, COF = 16.50, A = 0.246, R^2 = 0.995, n = 12; CA3, CF = 14.868, BW = 27.40, A = 0.091, R^2 = 0.809, n = 11; CA1, CF = 36.668, BW = 17.78, A = 0.055, R^2 = 0.982, n = 13. Comparisons for drug effect at each frequency, 2-way ANOVA with Bonferroni posthoc. Dentate: drug effect $F_{(1,148)} = 2.96$, $P = -.087$; frequency effect $F_{(7,148)} = 142.04$, $P < 0.001$. CA3: drug effect $F_{(1,206)} = 15.07$, $P < 0.001$; frequency effect $F_{(7,206)} = 3.27$, $P = 0.003$. CA1: drug effect $F_{(1,212)} = 13.22$, $P < 0.001$; frequency effect $F_{(7,212)} = 3.023$, $P = 0.005$. **D**. Differences between fits for PregS and ACSF for dentate (black solid line), CA3 (gray solid line), and CA1 (black dashed line). (Because of negative values for some differences, these data are plotted with a linear ordinate scale.)

Table 1

Parameter	CA3	CA1
EC	0.02014	0.01222
HN	1.1406	2.0084
S	32.9799	22.3137
$P_R 2$	0.04991	0.05442